









$$\begin{cases} C_0 = I \\ C_1 = i \operatorname{Re}(UI - cI) \\ C_2 = -2\widehat{D}^{(2)}I \\ C_3 = -i \operatorname{Re}U\widehat{D}^{(2)} + i \operatorname{Re}c\widehat{D}^{(2)} + i \operatorname{Re}U''I \\ C_4 = \widehat{D}^{(4)} \end{cases} \quad (43)$$

Different numerical methods can be used to solve equation (42). The simplest one consists in transforming it to a linear problem of larger dimension by forming the so-called companion matrices [20]. A companion matrix for equation (42) can be written as

$$\begin{pmatrix} -C_1 & -C_2 & -C_3 & -C_4 \\ I & 0 & 0 & 0 \\ 0 & I & 0 & 0 \\ 0 & 0 & I & 0 \end{pmatrix} - \alpha \begin{pmatrix} C_0 & 0 & 0 & 0 \\ 0 & I & 0 & 0 \\ 0 & 0 & I & 0 \\ 0 & 0 & 0 & I \end{pmatrix} \begin{pmatrix} \alpha^3 \varphi \\ \alpha^2 \varphi \\ \alpha^1 \varphi \\ \varphi \end{pmatrix} = 0 \quad (44)$$

This equation constitutes a generalized eigenvalue problem for  $\alpha$ , and can be solved efficiently by the QZ-algorithm [10].

## 7. RESULTS AND DISCUSSION

In Figures 2 and 3, the neutral stability curve and the mean flow velocity profile obtained in this study are compared with experimental results reported in the literature for impermeable wall ( $f_w=0$ ), [21]. A good agreement is observed. The neutral stability curve corresponds to  $c_i=0$ . It separates the unstable region ( $c_i>0$ ) and the stable region ( $c_i<0$ ), that remain inside and outside this curve.

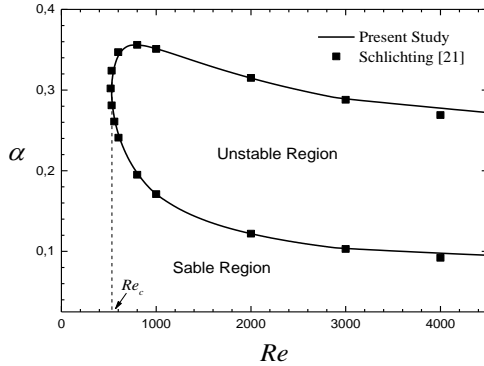


**Figure 2.** Neutral stability curve for impermeable wall:  
– numerical results, ■ experience [21]

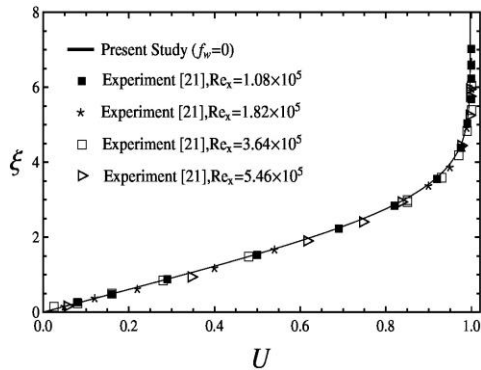


**Figure 3.** Velocity profile for impermeable wall:  
– numerical results, ■ experience [21]

Table 1 shows a comparison between obtained eigenvalues using various methods for the case  $Re=580$ ,  $\alpha=0.179$ ,  $y_w=20$  and  $N+1=44$ . The eigenvalues are given for the single unstable mode ( $c_i>0$ ). This comparison shows that the present numerical method is accurate.

**Table 1.** Eigenvalues of the Orr-Sommerfeld equation for laminar boundary layer ( $f_w=0$ ),  $Re=580$ ,  $\alpha=0.179$

Results	Eigenvalues
Present study	0.364552+0.0077791i
Grosch and Orszag [23]	0.364557+0.007773i
Zebib [24]	0.364143+0.007959i
Hatzivramidis and Ku [25]	0.364372+0.007884i
Xie et al. [26]	0.36455 +0.0077793i

### 7.1 Mean velocity profiles

Figures 4 and 5 present the mean velocity profiles obtained numerically by solving Equation (11) with the boundary conditions given in Equations (12)-(14) by standard Runge-Kutta method. Mathematically, suction or blowing are produced by imposing positive or negative values of wall stream function, respectively. We note that, the dimensionless velocity decreases with increasing the intensity of suction and increases with increasing the intensity of blowing. The intensity of suction or blowing is defined as the absolute value of the wall stream function.

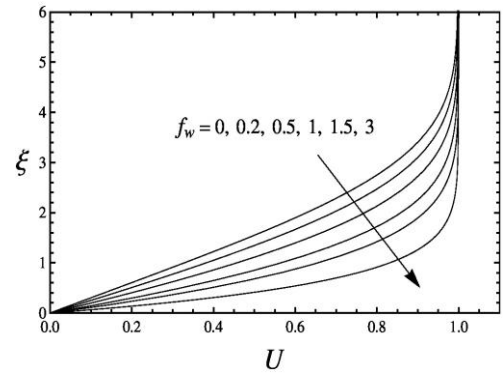


**Figure 4.** Mean velocity profile for wall suction ( $f_w>0$ )

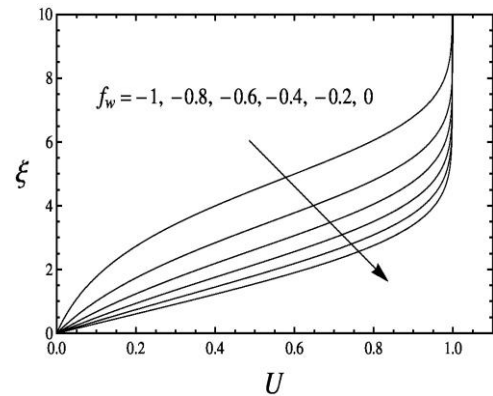


**Figure 5.** Mean velocity profile for wall blowing ( $f_w<0$ )

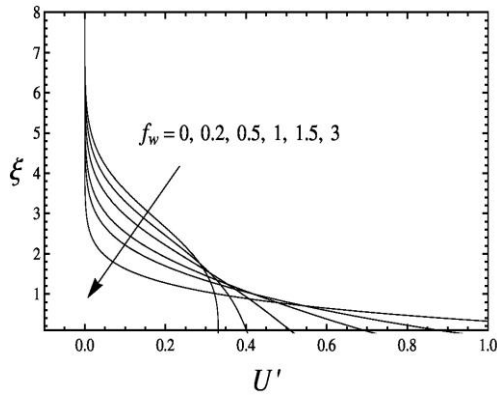


**Figure 6.** Velocity first-order derivative for wall suction

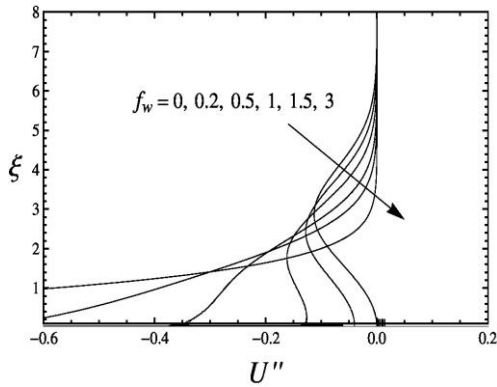


**Figure 7.** Velocity second-order derivative for wall suction

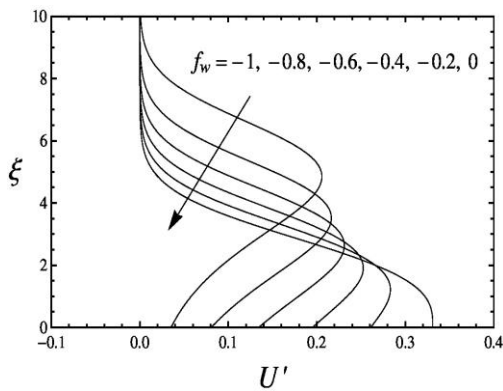


**Figure 8.** Velocity first order derivative for wall blowing

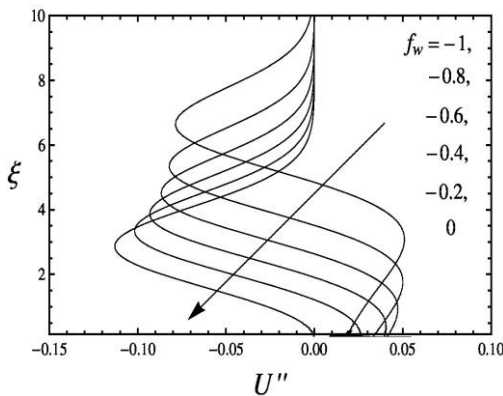


**Figure 9.** Velocity second-order derivative for wall blowing

The distributions of the first-order derivative  $U'$  and the second-order derivative  $U''$  of the velocity for the case of suction or blowing are shown in Figure 6 to 9, respectively. These quantities play an important role in the stability phenomena, and to achieve accurate results of the stability calculations, these profiles have to be produced with great accuracy.

## 7.2 Stability and transition characteristics of flow

Neutral stability curves are presented in the  $(Re, \alpha)$  plan for some values of the wall stream function, as can be seen in Figures 10 and 11.

In the neutral stability curves for suction, Figure 10, one sees a marked shifting to the right as the intensity of the suction increases. That is, the region of flow stability extends to higher Reynolds numbers as the suction becomes stronger.

In Figure 11, it is seen that increase in the intensity of blowing cause a marked left ward change of the curves, that is, toward lower Reynolds numbers. Thus, blowing is seen to be highly destabilizing.

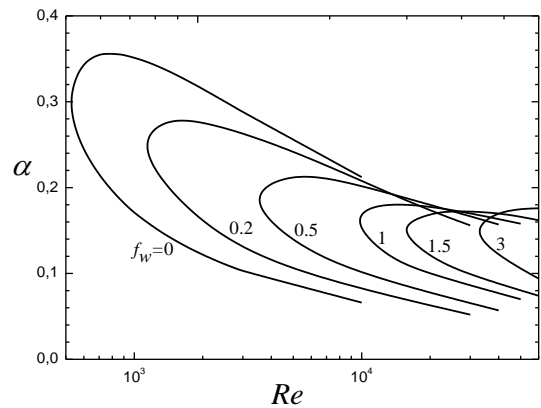


**Figure 10.** Neutral stability curves, for wall suction ( $f_w > 0$ )

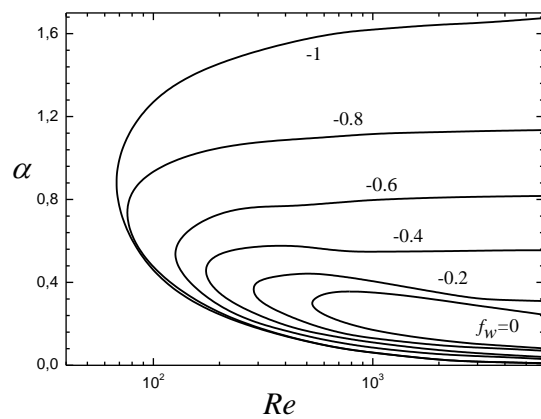


**Figure 11.** Neutral stability curves, for wall blowing ( $f_w < 0$ )

The summary of the stability calculations for two dimensional laminar external flow over a flat plate with wall suction and blowing submitted to linear two-dimensional disturbances is presented in Figure 12 and 13. Here the variation of the critical Reynolds number with suction and blowing is illustrated. As it is evident from this figures, the critical Reynolds number increases with increasing the intensity of suction or decreasing the intensity of blowing.

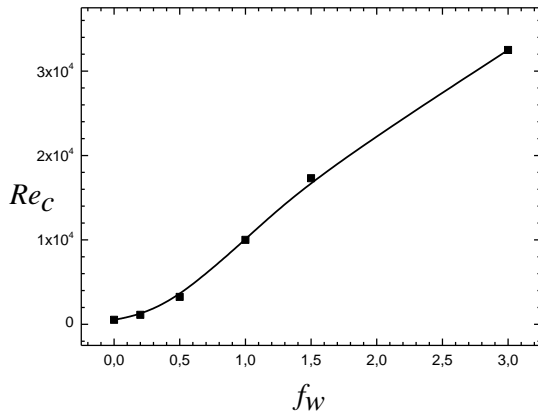


Figure 12. Critical Reynolds numbers for suction

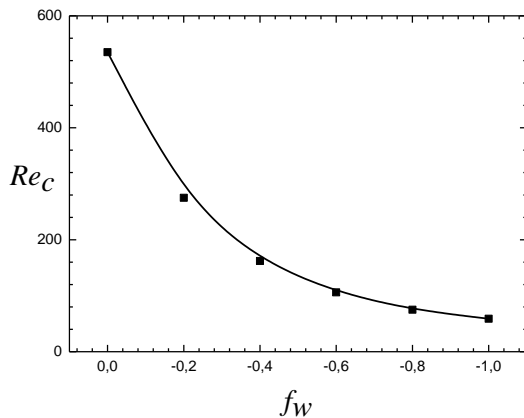


Figure 13. Critical Reynolds numbers for blowing

## 8. CONCLUSIONS

This study is focused on the temporal linear stability characteristics of laminar forced convection external flows along a horizontal permeable flat plate. For the mean flow, the similar boundary layer equations are used and solved numerically by a point-by-point Runge-Kutta-Verner method. The eigenvalue problem for the disturbance flow was solved numerically by the Chebyshev collocation spectral method. Neutral stability curves and critical Reynolds numbers are presented for different values of the wall stream function  $f_w$  ranging from 0.2 to 3 for wall suction and from -0.2 to -1 for wall blowing. The numerical solutions indicate the important role of the suction or blowing effect on the stability characteristics. The critical Reynolds number increases with increasing the intensity of suction or decreasing the intensity of blowing.

## REFERENCES

[1] M. E. Goldstein and L. S. Hultgren, "Boundary layer receptivity to longwave free-stream disturbances," *Annu. Rev. Fluid Mech.* vol. 21, pp. 137-166, 1989. DOI: [10.1146/annurev.fl.21.010189.001033](https://doi.org/10.1146/annurev.fl.21.010189.001033).

[2] H. W. Liepmann and G. L. Brown, "Active control of laminar-turbulent transition," *Journal of Fluid Mechanics*, vol. 118, pp. 201-204, 1982. DOI: [10.1017/S0022112082001037](https://doi.org/10.1017/S0022112082001037).

[3] T. Wiegand and H. Bestek, "Transition process of a wave train in a laminar boundary layer," *New Results*

in *Numerical and Experimental Fluid Mechanics*, vol. 60, pp. 397-404, 1997. DOI: [10.1007/978-3-322-86573-1\\_50](https://doi.org/10.1007/978-3-322-86573-1_50).

[4] J. Park and H. Choi, "Effects of uniform blowing or suction from a spanwise slot on a turbulent boundary layer flow," *Phys. Fluids*, vol. 11, no. 10, pp. 3095-3105, 1999. DOI: [10.1063/1.870167](https://doi.org/10.1063/1.870167).

[5] P. Ricco and F. Dilib, "The influence of wall suction and blowing on boundary-layer laminar streaks generated by free-stream vortical disturbances," *Physics of Fluids*, vol. 22, no. 4, pp. 1-13, 2010. DOI: [10.1063/1.3407651](https://doi.org/10.1063/1.3407651).

[6] K. Kim, M. K. Chung and H. J. Sung, "Assessment of local blowing and suction in a turbulent boundary layer," *AIAA J.*, vol. 40, no. 1, pp. 175-177, 2002. DOI: [10.2514/2.1629](https://doi.org/10.2514/2.1629).

[7] Z. Mehrez, M. Bouterra, A. El Cafsi, A. Belghith and P. Le Quere, "Enhancement of heat transfer in turbulent separated and reattached flow by a periodic perturbation," *International Journal of Heat and Technology*, vol. 27, no. 1, pp. 21-26, 2009.

[8] N. Ahmed and H. Kalita, "MHD oscillatory free convective flow past a vertical plate in slip-flow regime with variable suction and periodic plate temperature," *International Journal of Heat and Technology*, vol. 30, no. 2, pp. 97-106, 2012. DOI: [10.18280/ijht.300214](https://doi.org/10.18280/ijht.300214).

[9] K. Kim and H. J. Sung, "Effects of Periodic blowing from Spanwise slot on a turbulent boundary layer," *AIAA J.*, vol. 41, no. 10, pp. 1916-1924, 2003. DOI: [10.2514/2.1907](https://doi.org/10.2514/2.1907).

[10] S. Orszag, "Accurate solutions of Orr-Sommerfeld stability equation," *J. Fluid Mech.* vol. 50, pp. 689-703, 1971. DOI: [10.1017/S0022112071002842](https://doi.org/10.1017/S0022112071002842).

[11] J. J. Martinez and P. T. T. "Esperança, A Chebyshev collocation spectral method for numerical simulation of incompressible flow problems," *J. of the Braz. Soc. of Mech. Sci. & Eng.* vol. 29, no. 3, pp. 317-328, 2007. DOI: [10.1590/S1678-58782007000300013](https://doi.org/10.1590/S1678-58782007000300013).

[12] J. J. Dongarra, B. Straughan and D. W. Walker, "Chebyshev Tau-QZ algorithm methods for calculating spectra of hydrodynamic stability problems," *Appl. Numer. Math.*, vol. 22, no. 4, pp. 399-434, 1997. DOI: [10.1016/S0168-9274\(96\)00049-9](https://doi.org/10.1016/S0168-9274(96)00049-9).

[13] J. M. Melenk, N. P. Kirkner and V. Schwab, "Spectral Galerkin discretization for hydrodynamic stability problems," *Computing*, vol. 65, no. 2, pp. 97-118, 2000. DOI: [10.1007/s006070070014](https://doi.org/10.1007/s006070070014).

[14] S. C. Reddy, P. J. Schmid and D. Henningson, "Pseudospectra of Orr-Sommerfeld Operator," *SIAM J. Appl. Math.* vol. 53, no. 1, pp. 15-47, 1993. DOI: [10.1137/0153002](https://doi.org/10.1137/0153002).

[15] A. Hifdi, M. O. Touhami and J. K. Naciri, "Stabilité Linéaire d'Écoulements Symétrique Presque Parallèles en Canal," *C.R. Mécanique*, vol. 332, no. 10, pp. 859-866, 2004. DOI: [10.1016/S1631-0721\(04\)00161-5](https://doi.org/10.1016/S1631-0721(04)00161-5).

[16] J. P. Boyd, *Chebyshev and Fourier Spectral Methods*, New York: Dover Publications, 2000. DOI: [10.1007/978-3-642-83876-7U](https://doi.org/10.1007/978-3-642-83876-7U).

[17] C. Canuto, M. Y. Hussaini, A. Quarteroni and T. A. Zang, *Spectral Methods in Fluid Dynamics*, Berlin: Springer-Verlag, 1988. DOI: [10.1007/978-3-642-84108-8](https://doi.org/10.1007/978-3-642-84108-8).

[18] L. N. Trefethen, *Spectral Methods in MATLAB*, SIAM, 2000. DOI: [10.1137/1.9780898719598](https://doi.org/10.1137/1.9780898719598).

- [19] R. Peyret, "Spectral methods for incompressible viscous flow," *Applied Mathematical Sciences*, vol. 148, Springer-Verlag, New York, 2002. DOI: [10.1007/978-1-4757-6557-1](https://doi.org/10.1007/978-1-4757-6557-1).
- [20] A. V. Boiko, A. V. Dovgal, G. R. Grek and V. V. Kozlov, *Physics of Transitional Shear*, New York: Springer, 2012. DOI: [10.1007/978-94-007-2498-3](https://doi.org/10.1007/978-94-007-2498-3).
- [21] H. Schlichting and K. Gersten, *Boundary Layer Theory*, 8th Edition, Berlin Heidelberg: Springer-Verlag, 2000.
- [22] S. S. Motsa and Z. G. Makukula, "On spectral relaxation method approach for steady von Kármán flow of a Reiner-Rivlin fluid with Joule heating, viscous dissipation and suction/injection," *Cent. Eur. J. Phys.*, vol. 11, no. 3, pp. 363-374, 2013. DOI: [10.2478/s11534-013-0182-8](https://doi.org/10.2478/s11534-013-0182-8).
- [23] C. E. Grosch and S. A. Orszag, "Numerical solution of problems in unbounded regions: Coordinate transforms," *J. Comput. Phys.*, vol. 25, no. 3, pp. 273-295, 1977. DOI: [10.1016/0021-9991\(77\)90102-4](https://doi.org/10.1016/0021-9991(77)90102-4).
- [24] A. Zebib, "A Chebyshev Method for the solution of boundary value problems," *J. Comput. Phys.*, vol. 53, no. 3, pp. 443-455, 1984. DOI: [10.1016/0021-9991\(84\)90070-6](https://doi.org/10.1016/0021-9991(84)90070-6).
- [25] D. Hatzivramidis and H. C. Ku, "An integral Chebyshev Expansion Method for boundary-value problems of O.D.E. Type," *Comp. & Maths. with apps.*, vol. 11, no 6, pp. 581-586, 1985. DOI: [10.1016/0898-1221\(85\)90040-9](https://doi.org/10.1016/0898-1221(85)90040-9).
- [26] Ming-liang, L. Jian-zhong and X. Fu-tang, "On the hydrodynamic stability of a particle-laden flow in growing flat plate boundary layer," *J. Univ. Sci A: App. Ph. & Eng.*, vol. 8, no. 2, pp. 275-284, 2007. DOI: [10.1631/jzus.2007.A0275](https://doi.org/10.1631/jzus.2007.A0275)

## NOMENCLATURE

$c$	complex wave velocity
$C_i$	matrix coefficients, defined in Eq. (43)
$D$	the Chebyshev spectral differentiation matrix.
$d_{jk}$	elements of the Chebyshev spectral differentiation matrix Eq. (29)
$f$	non-dimensional stream function
$i$	complex number
$I$	identity matrix
$L$	length scale [m]
$N$	number of intervals in the Chebyshev domain
$P$	pressure [Pa m <sup>-2</sup> ]
$Re$	Reynolds number
$t$	time [s]
$T$	Chebyshev polynomials
$u$	axial velocity [m s <sup>-1</sup> ]
$U$	dimensionless axial velocity profile
$v$	normal velocity [m s <sup>-1</sup> ]
$X$	axial coordinate [m]
$x$	dimensionless axial coordinate
$Y$	normal coordinate [m]
$y$	dimensionless normal coordinate

## Greek symbols

$\alpha$	complex wave number
----------	---------------------

$\nu$	kinematic viscosity [m <sup>2</sup> s <sup>-1</sup> ]
$\psi$	wave disturbance
$\phi$	complex amplitude of the wave
$\omega$	$\omega = a(c_r + ic_i)$ , complex frequency
$\xi$	similarity coordinate
$\eta$	coordinates of the collocation points in the Chebyshev domain
$\rho$	mass density [kg m <sup>-3</sup> ]
$\tau$	dimensionless time
$\Psi$	stream function of state flow

## Subscripts and superscripts

'	differentiation with respect to $y$
$\sim$	fluctuating term
$-$	mean value
$k$	order of Chebyshev polynomials
$r$	real part
$i$	imaginary part
$w$	wall condition
$\infty$	free stream or outside border of boundary layer

## APPENDIX

In the two-dimensional formulation, equations (1)-(3), the instantaneous velocity components and pressure are

$$\begin{aligned} u &= \bar{u} + \tilde{u}, \\ v &= \bar{v} + \tilde{v}, \\ p &= \bar{p} + \tilde{p}, \end{aligned} \quad (1a)$$

where  $\bar{u}$ ,  $\bar{v}$ ,  $\bar{p}$  are the mean-flow terms and  $\tilde{u}$ ,  $\tilde{v}$ ,  $\tilde{p}$  the fluctuating terms.

Since  $\tilde{u}$ ,  $\tilde{v}$  and  $\tilde{p}$  are small, Eqs. (1) to (3) can be written as

$$\frac{\partial \tilde{u}}{\partial X} + \frac{\partial \tilde{v}}{\partial Y} = 0 \quad (2a)$$

$$\frac{\partial \tilde{u}}{\partial t} + \tilde{u} \frac{\partial \bar{u}}{\partial X} + \bar{u} \frac{\partial \tilde{u}}{\partial X} + \tilde{v} \frac{\partial \bar{u}}{\partial Y} + \bar{v} \frac{\partial \tilde{u}}{\partial Y} = -\frac{1}{\rho} \frac{\partial \tilde{p}}{\partial X} + \nu \left( \frac{\partial^2 \tilde{u}}{\partial X^2} + \frac{\partial^2 \tilde{u}}{\partial Y^2} \right) \quad (3a)$$

$$\frac{\partial \tilde{v}}{\partial t} + \tilde{u} \frac{\partial \bar{v}}{\partial X} + \bar{u} \frac{\partial \tilde{v}}{\partial X} + \tilde{v} \frac{\partial \bar{v}}{\partial Y} + \bar{v} \frac{\partial \tilde{v}}{\partial Y} = -\frac{1}{\rho} \frac{\partial \tilde{p}}{\partial Y} + \nu \left( \frac{\partial^2 \tilde{v}}{\partial X^2} + \frac{\partial^2 \tilde{v}}{\partial Y^2} \right) \quad (4a)$$

These equations can be simplified further by noting that all velocity fluctuations and their derivatives are of the same order of magnitude and by assuming that the mean flow velocity  $\bar{u}$  is a function of  $y$  only (parallel flow approximation [16]). So that: Eq.(1) gives

$$\bar{v} = 0 \quad (5a)$$

Using the dimensionless quantities defined as

$$x = \frac{X}{L}, y = \frac{Y}{L}, \tau = \frac{u_\infty t}{L}, \text{Re} = \frac{u_\infty L}{\nu} \quad (6a)$$



$$U = \frac{\bar{u}}{u_\infty}, u' = \frac{\tilde{u}}{u_\infty}, v' = \frac{\tilde{v}}{u_\infty}, p' = \frac{\tilde{p}}{\rho u_\infty^2} \quad (7a)$$

Equations (2a)-(4a) can be written as

$$\frac{\partial u'}{\partial x} + \frac{\partial v'}{\partial y} = 0 \quad (8a)$$

$$\frac{\partial u'}{\partial \tau} + U \frac{\partial u'}{\partial x} + v' \frac{\partial U}{\partial y} = -\frac{\partial p'}{\partial x} + \frac{1}{\text{Re}} \left( \frac{\partial^2 u'}{\partial y^2} + \frac{\partial^2 u'}{\partial y^2} \right) \quad (9a)$$

$$\frac{\partial v'}{\partial \tau} + U \frac{\partial v'}{\partial x} = -\frac{\partial p'}{\partial y} + \frac{1}{\text{Re}} \left( \frac{\partial^2 v'}{\partial x^2} + \frac{\partial^2 v'}{\partial y^2} \right) \quad (10a)$$

For the linear stability, the two-dimensional normal mode expansion is applied using the stream function ( $\psi$ ) formulation. Accordingly

$$\psi(x, y, \tau) = \varphi(y) e^{i\alpha(x-c\tau)} \quad (11a)$$

So, the fluctuating components of velocity are expressed as:

$$u' = \frac{\partial \psi}{\partial y} = \varphi' e^{i\alpha(x-c\tau)}, v' = -\frac{\partial \psi}{\partial x} = -i\alpha \varphi e^{i\alpha(x-c\tau)} \quad (12a)$$

And by substituting Eq.(9a) and eliminating the pressure in equations (8a)-(10a), we deduce the stability equation known as the Orr summerfeld equation:

$$\varphi'''' - 2\alpha^2 \varphi'' + \alpha^4 \varphi - i\alpha \text{Re}[(U-c)(\varphi'' - \alpha^2 \varphi) - U'' \varphi] = 0 \quad (13a)$$